



## Short communication

## Effect of deformation on electrical properties of carbon fibers used in gas diffusion layer of proton exchange membrane fuel cells

Nishith Parikh, Jeffrey Allen, Reza S. Yassar\*

Michigan Technological University, United States

## ARTICLE INFO

## Article history:

Received 18 March 2009

Received in revised form 16 April 2009

Accepted 17 April 2009

Available online 3 May 2009

## Keywords:

Carbon fiber

GDL

PEM

Kelvin resistance

Four-point probe

SEM

## ABSTRACT

In proton exchange membrane fuel cells, the stacks of anode, cathode, and membrane layers including gas diffusion layer (GDL) are held together by a compressive force applied through a bipolar plate. In this work, we studied the electrical properties of a carbon fiber of a GDL under deformation using four-point measurement methods inside a scanning electron microscope (SEM). We found out that through bending deformation the electrical resistivity of carbon fibers will be reduced. The drop in resistance during deformation may be the result of increasing conduction channels in the carbon fiber and parallel transport through them. Our finding offers a new insight on the effect of deformation on tuning the electrical properties of GDL materials.

© 2009 Elsevier B.V. All rights reserved.

## 1. Introduction

The gas diffusion layer (GDL) in fuel cells is a complex fibrous three-dimensional structure of carbon fibers. Such morphology constructs a porous material which allows the gases to pass through to the catalyst layer. Since carbon is conductive, it also facilitates the transport of electrons. Some of the theoretical studies [1,2] showed that under compression, the effect was significant enough to change the properties of current density distribution under the gas channels and the land areas. Meng and Wang [1] developed a three-dimensional, single-phase, isothermal numerical model to investigate effects of electron transport through the gas diffusion layer. It was found that the lateral electronic resistance of GDLs affected by the electronic conductivity, GDL thickness, and gas channel width, played a critical role in determining the current distribution and cell performance. Zhou and Liu [3] constructed a 3D fuel cell model incorporating the transport of electrons in the GDL and the catalyst layers to study the effects of the electrical resistance on current density distribution and cell power output. However, they found that the effect of GDL electronic resistance was negligible. They also reported that the thickness of GDL has minimal effect on the characteristics of the current density distributions.

\* Corresponding author at: Michigan Technological University, Mechanical Engineering-Engineering Mechanics, 1400 Townsend Drive, Houghton, MI-49931, United States. Tel: +1 906 4873581 fax: +1 906 4872822.

E-mail address: [reza@mtu.edu](mailto:reza@mtu.edu) (R.S. Yassar).

Recently, multiprobes based on scanning probe microscopy (SPM) techniques are being developed to characterize the electrical resistivity with nano to micron spacing. Takami et al. [4] have developed a twin probe scanning tunneling microscope with two probes driven independently [5]. Shiraki et al. report on a four-probe system operated in scanning electron microscope (SEM) where the surface conductance strongly depends on the probe spacing [6].

In polymeric fuel cells, the stacks of anode, cathode, and membrane layers including gas GDL are held together by a compressive force applied through a bipolar plate [7]. The majority of the studies are focused on the effect of GDL compression on gas permeability and contact resistance [4]. In the literature, there is not much information about the electrical properties of GDL under deformation. In this study, we conducted the deformation of a carbon fiber of a GDL using a four-nanomanipulator system inside a SEM and measure the current–voltage response in the fiber. To the authors knowledge this is the first study on the effect of deformation on electrical properties of GDL materials.

## 2. Experimental procedure

The carbon fibers were taken out from a GDL sample which was obtained from Ballard's AvCarb™ Grade-P75T carbon fiber paper. AvCarb P75T is a polyacrylonitrile-based carbon fiber paper manufactured utilizing Ballard's exclusive AccuCarb continuous carbonization process. A typical method for measuring the electrical properties of materials is based on two-probe measurements. A problem that occurs when using a two-probe setup is that the

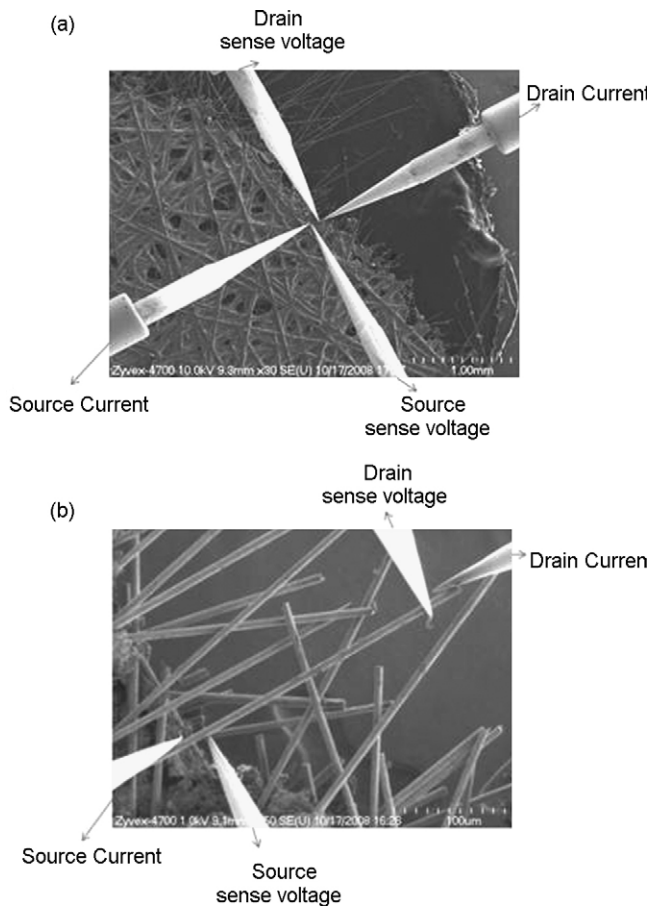


**Fig. 1.** (a) SEM image of four nanomanipulators independently driven in a SEM chamber. The tips are separated as far as about 1 mm in the top panel, while they are brought together to within a distance less than 10 nm spacing in the other panels. Outermost probes are source and drain current and innermost is source and drain sense voltages. (b) SEM image of nanomanipulator tips during electrical measurements of a carbon fiber with no bending deformation.

voltage is measured not only across the resistance in question, but includes the resistance of the leads and contacts as well. When using an ohmmeter to measure resistances above a few ohms this added resistance is usually not a problem. However, when measuring low resistances or when contact resistance may be high, obtaining accurate results with a two-wire measurement could impose large errors in the measurements. To overcome this shortcoming, four-point measurements [8] were employed in this study. In this configuration, an additional set of probes is used for sensing and since negligible current flows in these probes, only the voltage drop across the device under test will be measured.

The electrical properties were directly measured by a four-probe nanomanipulation system (S-100) produced by Zyvex inside a Hitachi S-4700 field emission SEM. Fig. 1a and b shows the arrangement of nanomanipulators and a carbon fiber in the four-probe configuration, respectively, used for this investigation. The four-point probe setup used consists of four equally spaced tungsten metal tips with finite radius. Each tip is supported by springs on the other end to minimize sample damage during probing. The four metal tips are part of an auto-mechanical stage which travels up and down during measurements. A SEM image of a carbon fiber with no bending deformation is shown in Fig. 1b. The nanomanipulator system offered 5 nm movement precision with probe tip diameters less than 20 nm, and current-measuring capability down to 1 pA. The linear array configuration of these four probes is chosen, i.e. the two probes perform as current source and drain, while the electri-

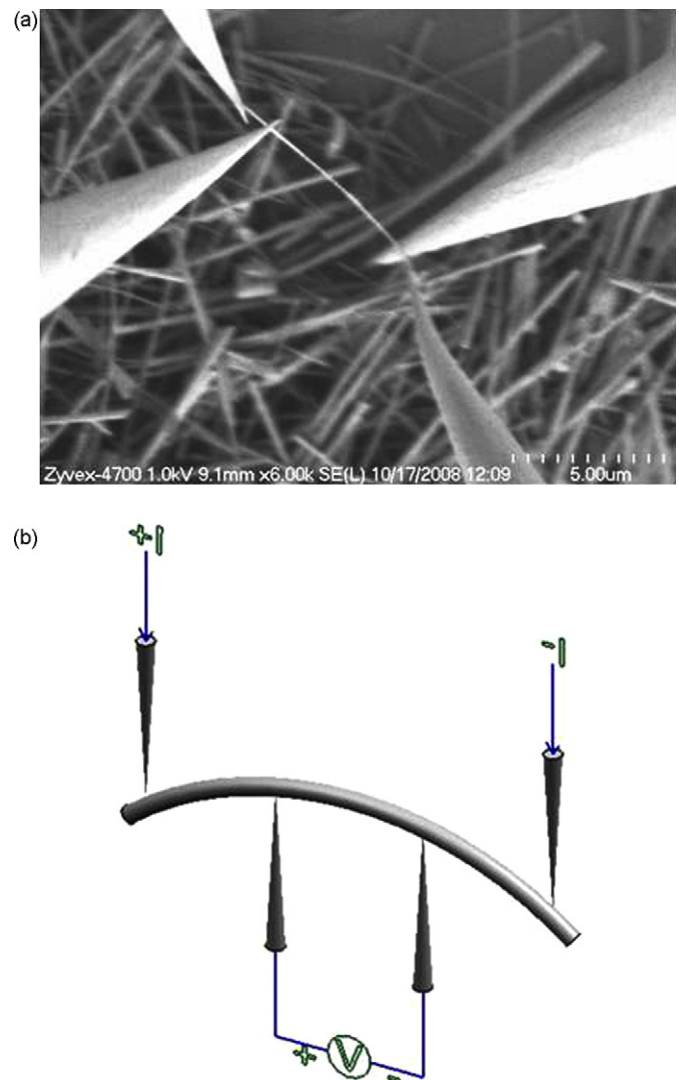


**Fig. 2.** SEM image of a carbon fiber during bending (a) the nanomanipulator setup, and (b) the schematic of current and voltage detection in the bended fiber.

cal potential drop is measured across the inner ones. The outermost probes are for source current and drain current, and the innermost are for source sense voltage and drain sense voltage, respectively. The source current, drain current, source sense voltage and drain sense voltage are indicated in Fig. 1a and b. Initially, electric tip processing (ETP) [9] was employed to clean and/or sharpen the probe tips in the SEM chamber by passing the electrical current between the probes. The ETP includes bringing two probes into close proximity, and biasing the probes at different DC-voltages such that any oxide or other dielectric or contaminant that is interposing the two probe tips breaks down.

### 3. Results and discussion

The SEM images of a carbon fiber during bending experiments are shown in Fig. 2a. The typical in-line setup with four probes (Fig. 2b) involves driving a current between the two outer probes while measuring the resulting voltage drop between the inner two probes using a high-impedance voltmeter ( $>10 \Omega G$  in our case) so that very little current is drawn. This yields a current–voltage ( $I$ – $V$ ) curve dependent on the separation  $d$  between the probes. For these measurements a single carbon fiber with a length of about 325  $\mu m$  was selected and lifted with nanomanipulator to a certain height

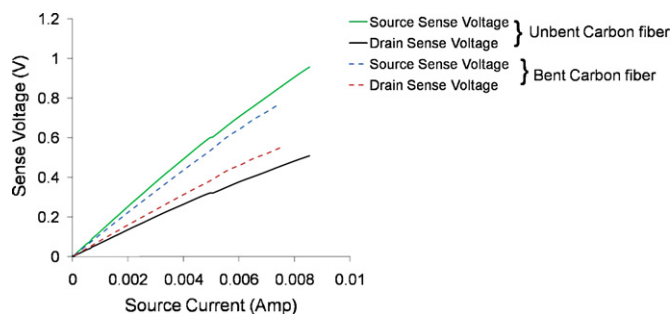


Fig. 3. Source current–sense voltage characteristics for unbent carbon fiber and during the bending for the same carbon fiber.

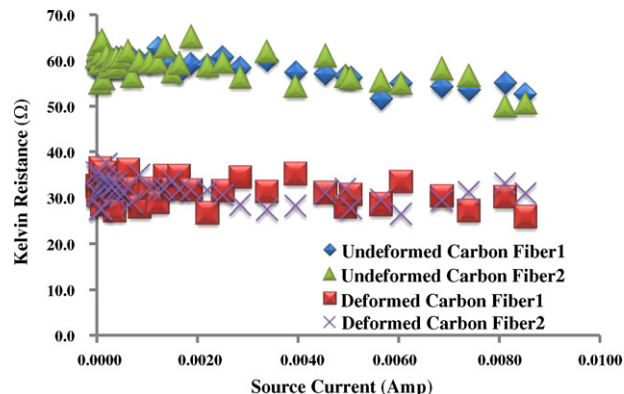


Fig. 4. Kelvin resistance–source current characteristics for unbent carbon fibers and after the bending deformation.

for measurement. Using the nanomanipulator setup, a single fiber was placed between the probes in a way that allowed the bending of carbon fibers. Initially the carbon fiber was hold firmly with three of nanomanipulators (source current, drain current, and drain sense voltage probes). Then by upward movement of source sense voltage probe the bending process was accomplished. It should be noted that the carbon fibers were extremely rigid and the bending of carbon fibers was not successful always. We estimated the amount of force required to bend the fiber (for small bending angles) using Euler formula:

$$F_{\text{Euler}} = \frac{\pi^2 EI}{L^2} \quad (1)$$

where  $E$  is the Young's modulus of carbon fiber and assumed to be 221 GPa [10].  $I$  is the moment of inertia taken as  $I = \pi d^4/64$ , where  $d$  is the diameter of carbon fiber ( $\sim 5 \mu\text{m}$ ).  $L$  is the length of carbon fiber ( $\sim 325 \mu\text{m}$ ). Using these values, the bending force was calculated to be  $\sim 6.32 \times 10^{-4}$  N.

The  $I$ – $V$  characteristics of a carbon fiber before bending and after bending experiments are shown in Fig. 3. From the graph, we observe that source sense voltage in both bent and unbent conditions are almost similar, while there is significant difference in drain sense voltage for unbent and bent carbon fiber. Since negligible current flows through these sense probes, only the voltage drop

across the device under test is measured. That is known as Kelvin resistance. It is calculated as follows:

$$\text{Kelvin resistance} = \frac{V_{\text{source\_sense}} - V_{\text{drain\_sense}}}{\text{source current}} \quad (2)$$

The source current versus Kelvin resistance is shown in Fig. 4. From the figure we observe that the Kelvin resistance decreases under bending deformation. This observation was consistent for several tested carbon fibers. The raw data for two carbon fibers, designated as carbon fiber 1 and carbon fiber 2, are plotted in Fig. 4 to demonstrate such consistency. It is not clear for the authors the exact mechanism by which the current increased. While the structure of carbon fibers is different from multiwalled carbon nanotube but similar observation has been made for multiwall carbon nanotubes [11]. It was observed that the bent nanotube resulted in substantial decrease in electrical resistance. The drop in resistance during bending was attributed to the increase of number of conduction channels inside the nanotube and parallel transport through them. Our finding offers a new insight on the effect of deformation on tuning the electrical properties of GDL materials. It should be noted that to connect the present study to practical fuel cell application, it is necessary to study the effect of measured fiber resistance on the in-plane electrical resistance under bending conditions.

#### 4. Conclusion

In this work, we studied the electrical properties of GDL carbon fibers under deformation using an *in situ* four-point measurement method inside a SEM. We found out that by bending the electrical resistivity of carbon fibers will be reduced. The drop in resistance during deformation may be the result of increasing conduction channels in the carbon fiber and parallel transport through them. Our finding offers a new insight on the effect of deformation on tuning the electrical properties of GDL materials.

#### Acknowledgements

This work was supported by the Department of Energy (DOE) under the grant DE-FG36-07G017018. We thank General Motor for providing us the gas diffusion layer sample. The authors also thank Zyvex, USA for the use of their scanning electron microscopy and nanomanipulator system.

#### References

- [1] H. Meng, C.Y. Wang, J. Electrochem. Soc. 151 (2004) A358–A367.
- [2] B.R. Sivertsen, N. Djilali, J. Power Sources 141 (2005) 65–78.
- [3] T. Zhou, H. Liu, J. Power Sources 161 (2006) 444–453.
- [4] K. Takami, M. Akai-Kasaya, A. Saito, M. Aono, Y. Kuwahara, Jpn. J. Appl. Phys. 44 (2005) L120–L122.
- [5] C.L. Petersen, F. Grey, I. Shiraki, S. Hasegawa, Appl. Phys. Lett. 77 (2000) 3782.
- [6] I. Shiraki, T. Nagao, S. Hasegawa, C.L. Petersen, P. Boggild, T.M. Hansen, F. Grey, Surf. Rev. Lett. 7 (2000) 533–537.
- [7] T. Hottinen, O. Himanen, S. Karvonen, I. Nitta, J. Power Sources 171 (2007) 113–121.
- [8] F.M. Smits, Bell System Tech. J. 37 (1958) 711.
- [9] C. Baur, R.J. Folaron, A. Hartman, P.C. Foster, J.C. Nelson, R.E. Stallcup, EP Patent 1,566,647 (2007).
- [10] X. Wang, S. Wang, D.D.L. Chung, J. Mater. Sci. 34 (1999) 2703–2713.
- [11] V. Semet, V.T. Binh, D. Guillot, K.B.K. Teo, M. Chhowalla, G.A.J. Amaratunga, W.I. Milne, P. Legagneux, D. Pribat, Appl. Phys. Lett. 87 (2005) 223103–223105.